JOURNAL OF MATERIALS SCIENCE 10 (1975) 279–289

Indexing Kossel patterns

NEIL HARRIS*
Department of Metallurgy and Materials Science, University of Liverpool, UK

Procedures for the indexing of Kossel patterns are fully explained with reference to the use of pattern symmetry, diffraction curve intensity, line curvature and Kossel curve intersections. The indexing methods are illustrated by analysis of a face centred cubic pattern. General application of the concepts described here to the more difficult indexing problems experienced with hexagonal and orthorhombic crystal structures is included.

1. Introduction

Although X-ray divergent beam (Kossel) diffraction has been understood for many years and applied to a large variety of crystallographic problems, very little has been written on the subject of indexing Kossel patterns. Investigations have been largely confined to studies with cubic crystals where indexing is straightforward. When, however, we wish to apply the technique to less simple crystal structures it is useful to consider some general guides to the indexing of these patterns. Since it is not clearly set down what indexing techniques have been used by authors of earlier papers on Kossel diffraction it is the purpose of this paper to state the methods that have been developed and employed in our laboratory for this purpose.

The information in a single Kossel pattern is large and the pattern appears at first sight most complicated; yet the indexing of such patterns is not difficult and the results are reliable simply because it is possible for any deductions to be cross-checked in several ways. The indexing problem is, therefore, by no means as great as in the case of Debye-Scherrer patterns from low symmetry crystals, and overlapping of lines from planes with similar spacing but different Miller indices are impossible. Kossel curves are indexed by consideration of one or other, or a combination of the pattern symmetry, relative intensity, curvature, and their intersections one with another. The symmetry is dependent on the crystal structure alone, and the identification of symmetry elements not only increases knowledge of the crystal structure but also indicates certain crystallographic directions. Relative intensities of the diffraction curve are complex functions of a number of parameters, chief among these being the structure factor, and consideration of this alone will be sufficient for our purposes. The curvature depends on the Bragg angle and increases with decreasing lattice spacing. Kossel curve intersections depend on symmetry and Bragg angles in a manner which will be described below. Fig. 1a is a typical back-reflection Kossel pattern and Fig. 1b is a drawing including some, but not all, of the Kossel curves present in Fig. 1a. These will serve to illustrate many of the indexing techniques described here. The fully indexed pattern is shown in Fig. 1c.

2. Symmetry

The symmetry is readily revealed in Kossel patterns because each plane of a type with non-zero structure factor diffracts its own Kossel cone and the position of each curve in the pattern depends on the crystallographic direction of the normal to the diffracting plane. "Mirror lines" are easily drawn on a pattern as in Fig. 1b but it must be noted that the pattern on one side of such a line will be a distorted image of the pattern on the opposite side due to the gnomonic projection of the diffraction pattern onto the flat plane of the recording film. Intensities of the Kossel curves may also differ on opposing sides of a "mirror line". Although, however, the two sides may not be exact mirror images every point on one side of a "mirror line" corresponds to a similar point on the other side and in this sense they are easily recognizable features of a Kossel pattern. Several "mirror lines" have been drawn in Fig. 1b and it is clear in Fig. 1a that although curve 3 is the "mirror" of curve 4 in line BB', the intensities of the two lines are very different.

*Present address: University of London Careers Advisory Service, 50 Gordon Square, London, UK

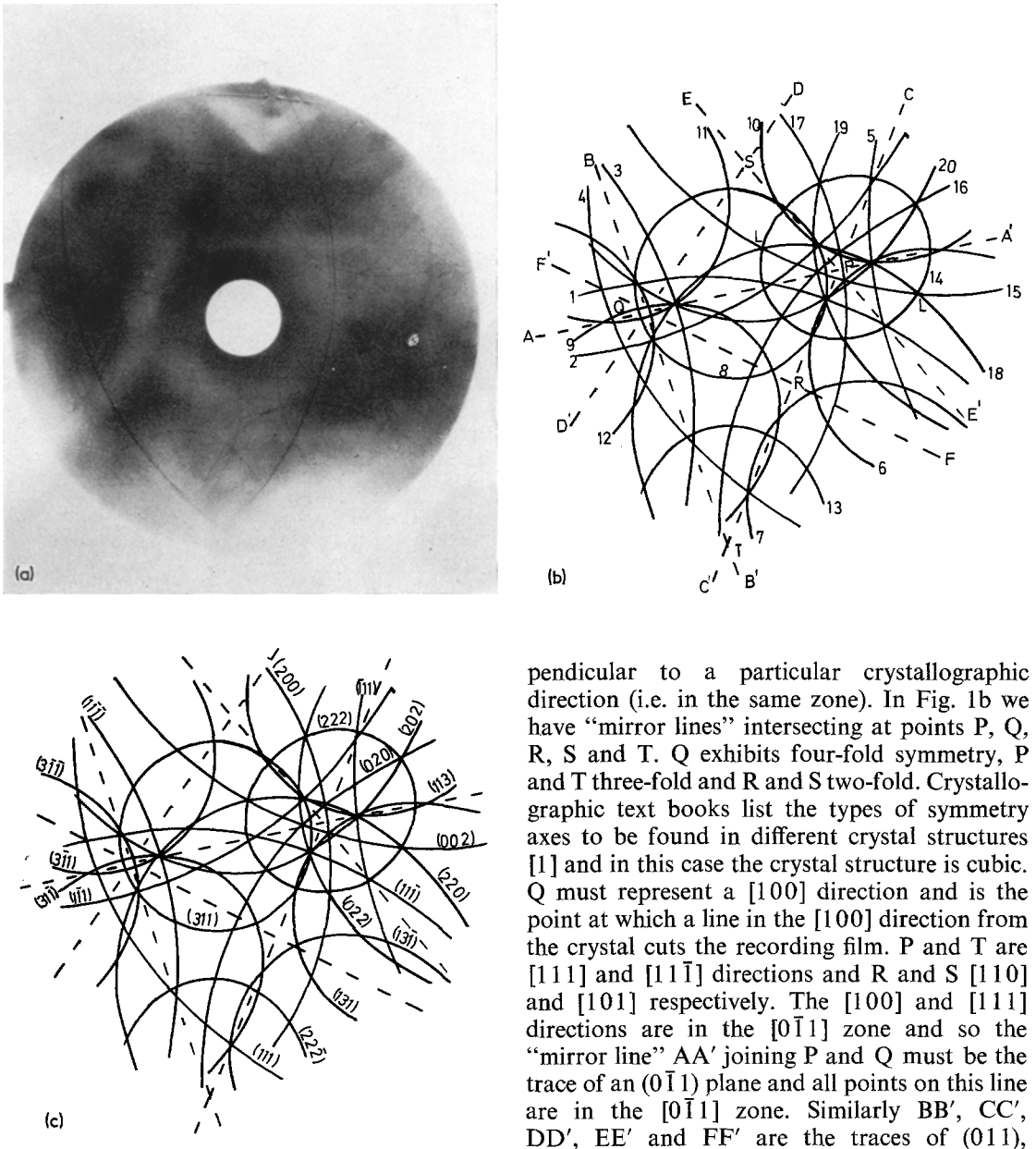

Figure 1 Analysis of austenite Kossel pattern.

Similarly, the regions on either side of line AA′ in the vicinity of point Q are not exact mirror images but exhibit some distortion due to the projection.

Crystallographically these lines are very significant. They meet at points of symmetry and they represent the projection of particular sets of crystallographic planes onto the recording film. All points on a single "mirror line" are perpendicular to a particular crystallographic direction (i.e. in the same zone). In Fig. 1b we have "mirror lines" intersecting at points P, Q, R, S and T. Q exhibits four-fold symmetry, P and T three-fold and R and S two-fold. Crystallographic text books list the types of symmetry axes to be found in different crystal structures [1] and in this case the crystal structure is cubic. Q must represent a [100] direction and is the point at which a line in the [100] direction from the crystal cuts the recording film. P and T are [111] and [11$\bar{1}$] directions and R and S [110] and [101] respectively. The [100] and [111] directions are in the [0$\bar{1}$1] zone and so the "mirror line" AA′ joining P and Q must be the trace of an (0$\bar{1}$1) plane and all points on this line are in the [0$\bar{1}$1] zone. Similarly BB′, CC′, DD′, EE′ and FF′ are the traces of (011), (1$\bar{1}$0), (010), (10$\bar{1}$) and (001) planes respectively, and points on these lines are in the corresponding zones.

Crystal structures which exhibit less symmetry have fewer "mirror lines" and fewer symmetry points. It is noteworthy that in the cubic case the whole pattern is recorded in the [100], [111] [110] triangle. This is triangle PQR in Fig. 1b and the pattern in triangles PQS and RQT is a repetition of the same pattern. For non-cubic crystals, however, a much larger solid angle must be recorded to ensure that the whole pattern is

observed and this has a bearing on the camera design.

Continuing further with the indexing of the pattern Fig. 1b symmetrically related Kossel curves have similar Miller indices and are diffracted by planes of the same family. Curves 1 and 2 are symmetrically related through mirror line AA′ and curves 1 and 5 through mirror line EE′. Because Q is a point of four-fold symmetry curves 3 and 4 must also be diffracted by planes of the same family as curves 1 and 2. We have found that curves 1 to 5 are all from planes of the same type and study of the other curves reveals that there are curves from five different families of lattice planes. Four other families of planes are represented by curves 6 to 12, 13 and 14, 15 to 17 and 18 to 20. Some curves are crossed by "mirror lines" in such a way that one half of the curve is reflected across the line. Examples of this are the reflection of curve 8 in AA′ and curve 14 in AA′, CC′ and EE′. Another important case is the reflection of curve 4 in AA′ and CC′. Such curves have their centres on the lines concerned, or if there are two such lines more precisely at their intersection. The significance of this is that the diffracting planes for those curves must be in the zone dictated by the "mirror line". This condition introduces limitations on the Miller indices of curves centred on the "mirror lines" and these are tabulated for Fig. 1b in Table I. All curves on AA′ are in the $[0\bar{1}1]$ zone and their Miller indices must satisfy the rule that the scalar product $(hkl).(0\bar{1}1) = 0$ which is only satisfied if $k = l$. Thus curve 14 must obey these rules for AA′, CC′, EE′ and have Miller indices $h = k = l$; curve 4 must obey them for AA′ and EE′ so that $h = k = l$ for this line also. Curve 8 is cut symmetrically by line AA′ and its Miller indices must satisfy the condition $k = l$.

A great deal has been achieved by consideration of symmetry alone, but it is not possible to complete the indexing procedure without the consideration of at least one other of the indexing aids available.

3. Intensity

It is unusual for Kossel curves to be recorded from families of planes other than those with the highest structure factors. When we consider such structures as body or face centred cubic or hexagonal crystals there are a large number of planes excluded from diffraction by having structure factors of zero. An additional factor

TABLE I

Mirror line	Trace of planes	Conditions of Kossel curves with centre of symmetry on the mirror line
AA′	$(0\bar{1}1)$	$k = l$
BB′	(011)	$k = -l$
CC′	$(1\bar{1}0)$	$h = k$
DD′	(010)	$k = 0$
EE′	$(10\bar{1})$	$h = l$
FF′	(001)	$l = 0$

included in Kossel curve intensity calculation is $1/\sin 2\theta$ where θ is the Bragg angle and this results in curves with high or low Bragg angles being more intense than those with Bragg angles near to 45°. A complete analysis of intensity factors cannot be given here and is not a necessary prerequisite for indexing to be carried out successfully. When the crystal has previously been the subject of Debye-Scherrer diffraction experiments it is a simple matter to list the planes diffracting the most intense lines and to look first for these in the Kossel pattern.

If we consider the pattern in Fig. 1 it is cubic and there are curves recorded from five different families of lattice planes. We set out in Table II the possible Miller indices of these planes for different cubic crystal structures when lattice planes with zero structure factor are omitted.

TABLE II First five diffracting planes in cubic systems

Simple cubic	bcc	fcc
(100)	(110)	(111)
(110)	(200)	(200)
(111)	(211)	(220)
(200)	(220)	(311)
(210)	(310)	(222)

In the case of the pattern under consideration we have seen in Section 2 that two curves are centred on the point of three-fold symmetry P and have Miller indices $h = k = l$. These two curves have different curvature and therefore have different Miller indices. The crystal must, therefore, be face centred cubic in structure and the Miller indices of these two curves (111) and (222). If we return to Table I it is now seen that curves 1 to 5 are diffracted from {111} planes and curves 13 and 14 from {222} planes. Curve 18 surrounds R and curves 18 to 20 are from {220} planes. Curve 8 is not associated with any

symmetry point and is from {311} as are all the curves 6 to 12. Finally curve 17 has AA′ as major axis, surrounds Q and is of type {200}.

4. Line curvature

It is well known that Kossel diffraction cones have semi-apex angles $\alpha = (90 - \theta)$ and that a Kossel curve is the conic section formed by the intersection of such a cone with the flat recording film. Thus for any specified specimen to film distance, the cone apex being at the specimen, the curvature of the recorded Kossel curves is dependent on the Bragg angle and the lattice spacing. Decreasing the lattice spacing increases the Bragg angle, decreases the semi-apex angle of the Kossel cone and thus increases the curvature of the Kossel curve. For cubic crystals the sum of the Miller indices will, therefore, be higher for curves with high curvature and low radius. This is not always so when non-cubic crystals are considered. When the specimen to film distance is fixed we may draw a graph indicating the position and curvature of a Kossel curve in the pattern assuming a given Bragg angle. The position and curvature also depend on the normal direction of the crystal plane and graphs can be drawn for a sequence of values of this parameter. Such graphs, one of which is seen in Fig. 2, have been plotted by Rowlands and Bevis [2] and are directly equivalent to Grenninger charts used for the analysis of Läue patterns. With a set of these charts (and a different chart is necessary for each family of planes represented), it is possible to determine an approximate value for the Bragg angle of each curve in the pattern. The normal directions are also quickly read off from the co-ordinates on the chart and the poles plotted onto a stereographic projection. Numbers at the curve midpoints are the angular distances of the pole from the centre of the pattern and numbers at the circumference are the angular rotation of the chart from a fixed direction. This method of indexing is effective if the specimen–film distance is fixed and one has charts for each of the Bragg angles occuring in the pattern. The pole position is simply found by fitting the Kossel curve to a curve on the chart and the co-ordinates are noted.

Another stereographic projection method is that of Peters and Ogilvie [3] in which a gnomonic net is constructed and superimposed on the pattern. The co-ordinates of three or more

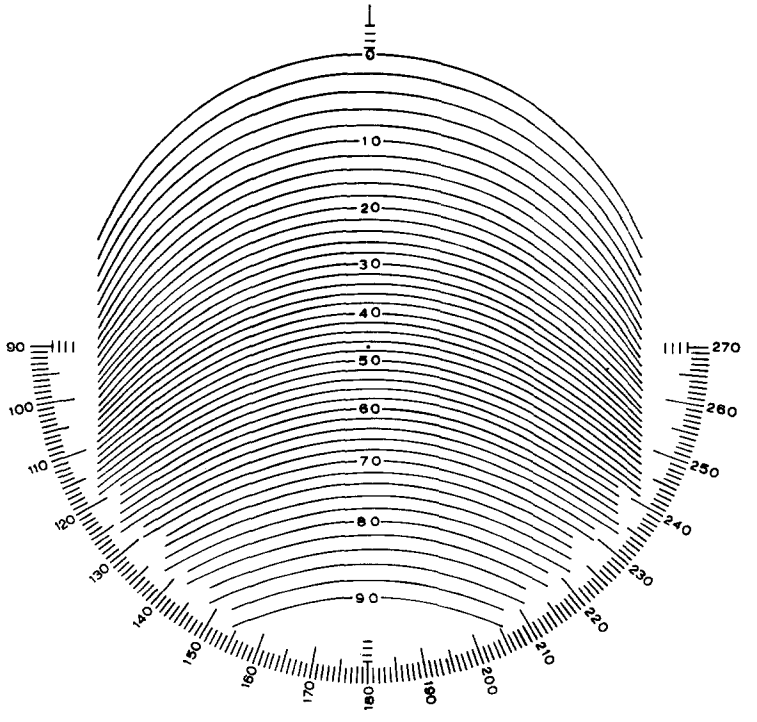

Figure 2 Rowlands-Bevis chart

points on each Kossel curve are then plotted onto a stereographic net where the curves appear as circles. At least three points on each curve are required for the geometrical construction necessary to draw the circle on the stereographic projection. Accurate construction of the circle is only achieved if the points are well separated from one another. This method again results in the poles of the diffracting curves being plotted on the stereographic net and the Bragg angles determined.

Both of these methods can yield the Bragg angle and pole position to a precision of $\pm 2°$. Indexing is then achieved by consideration of Bragg angles, the angles between poles and the pattern symmetry. These techniques are capable of solving the indexing problems of the most difficult Kossel patterns if symmetry is also considered.

5. Intersections

One of the most readily appreciated features of any Kossel pattern is that the Kossel curves frequently intersect one another. In some cases more than two Kossel curves intersect at the same point and these will be referred to as multiple intersections. All intersections, whether between two curves or multiple, can be studied to give us information about the crystal concerned, and their crystallographic basis can be of considerable benefit when indexing patterns from cubic crystals.

It was shown in Section 2 that curves could be distinguished as belonging to lattice planes of the same family by symmetry considerations. The same conclusions can be drawn by counting the number of intersections on each curve. All curves in the same family are symmetrically related and have an identical number of intersections with other curves. It is possible that curves from different families of lattice planes may display the same number of intersections but such an occurrence is fortuitous. The chief difficulty encountered with this method is that whole curves are rarely recorded, but the total number of intersections can often be deduced from symmetry considerations. The numbers of intersections in which the curves in Fig. 1a participate are given in Table III. An easier method is to count the number of multiple intersections on a given curve since these are less numerous, and these are also given in the table. Study of multiple intersections has other benefits which will be discussed later. In this example there are no quintuple intersections as are often found in Kossel patterns from bcc crystals.

TABLE III

Miller indices of curve	Total intersection points	Triple intersection points
(111)	30	12
(200)	48	16
(220)	38	14
(311)	24	4
(222)	18	6

The conditions for intersections have been established by Kossel [4] and more recently by MacKay [5] and Frazer and Arrhenius [6]. Intersections are of three types illustrated in Fig. 3, and although the diagram has been re-

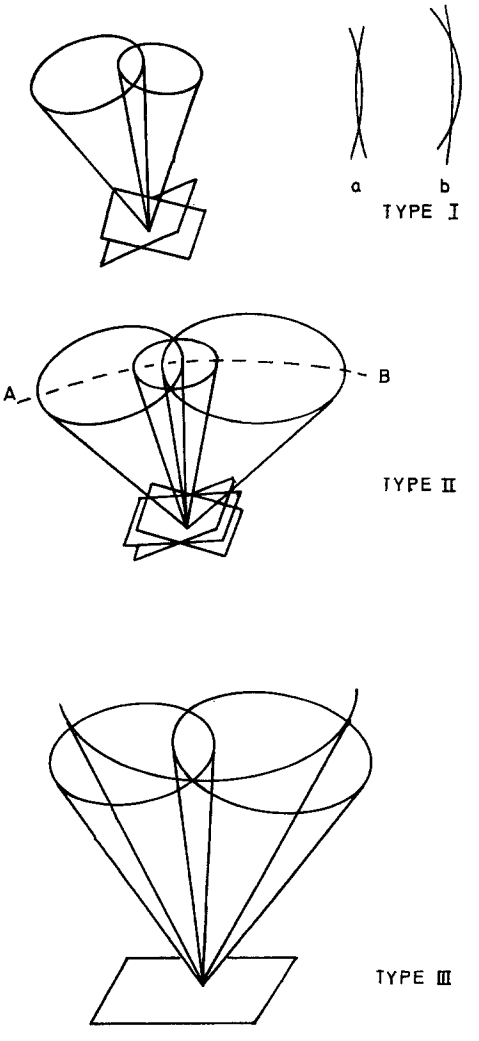

Figure 3 Kossel cone intersections.

stricted to three planes for ease of drawing, more planes can be involved in each case.

Type I intersections form the typical lens shape which is the basis for some lattice parameter determination methods [7]. If α_1 and α_2 are the semi-apex angles of each cone and ϕ_{12} is the angle between the plane normals (i.e. cone axes) then for type Ia intersections $\alpha_1 + \alpha_2 > \phi_{12}$ and for type Ib $|\alpha_1 - \alpha_2| > \phi_{12}$. Type III intersections include three or more diffraction curves. They are known as "accidental" intersections because they only occur at one wavelength–lattice spacing ratio and unlike type II intersections they do not exhibit symmetry characteristics. These intersections are very sensitive to the magnitude of the lattice parameter and extremely useful for precise lattice parameter determination [8].

Type II intersections are more important for indexing because they occur between Kossel curves from well defined sets of lattice planes. They are often referred to as invariant, geometrical, persistent or inevitable because they are not sensitive to lattice parameter or wavelength changes but depend on the crystal structure. Points L in Fig. 1b indicate one pair of intersections of this type. There is a symmetry associated with these intersections and it is always possible to draw one line which is the major axis of all the curves concerned. This is the line AB in Fig. 3. As we have seen in Section 2, this means that all the planes contributing to such an intersection are in the same zone and their Miller indices must obey the zone law. Again symmetry dictates that these intersections must occur in pairs and this identifies them from type III intersections which appear singly.

MacKay [5] produced a good analysis of multiple intersections but his conclusions were inaccurate. It is therefore necessary to reiterate his argument briefly if it is to be of use for our purposes here. If one takes the apex of a Kossel cone as the origin and draws a sphere around this point with unit radius then the plane in which the Kossel cone intersects the sphere is called the Kossel plane and the distance of this plane from the origin is $\lambda/2d$. This is shown in Fig. 4a. If the crystallographic axes are taken as co-ordinate axes the equation of a Kossel plane can be written as follows:

$$\frac{hx}{a} + \frac{ky}{b} + \frac{lz}{c} = \frac{\lambda}{2d^2} = Q \qquad (1)$$

where (hkl) are the Miller indices, (a, b, c) the lattice parameters, d the plane spacing and λ the wavelength. This equation is for orthogonal axes only.

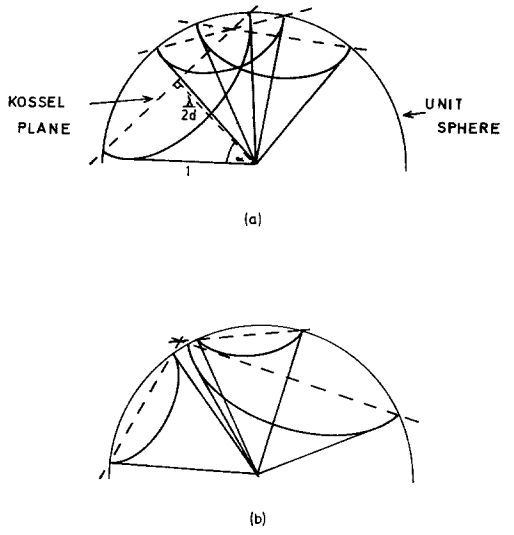

Figure 4 Kossel plane intersections.

A persistent multiple intersection occurs when three or more Kossel planes meet in a line within the unit sphere as in Fig. 4a. The condition for three planes as in Equation 1 to meet in a line is that there is no single solution to the three simultaneous equations and the following four determinants are zero.

$$\begin{vmatrix} h_1k_1l_1 \\ h_2k_2l_2 \\ h_3k_3l_3 \end{vmatrix} = \begin{vmatrix} h_1k_1Q_1 \\ h_2k_2Q_2 \\ h_3k_3Q_3 \end{vmatrix} = \begin{vmatrix} h_1Q_1l_1 \\ h_2Q_2l_2 \\ h_3Q_3l_3 \end{vmatrix} = \begin{vmatrix} Q_1k_1l_1 \\ Q_2k_2l_2 \\ Q_3k_3l_3 \end{vmatrix} = 0 \qquad (2)$$

These stringent conditions make it possible to list the Kossel planes from any given crystal structure that will meet in a line. The fact overlooked by MacKay is that if they meet in a line outside the unit sphere the Kossel curves do not overlap and multiple intersections are not recorded. Such is the case with the curves (3 1 1) (2 0 0) and ($\bar{1}$ 1 1) in Fig. 1c which obey the condition in Equation 2 but do not intersect because the Kossel planes meet in a line outside the unit sphere. This situation is illustrated in Fig. 4b.

It is, nevertheless, useful to list possible multiple intersections. For this purpose a hypothetical crystal was considered and a

computer program was written to investigate every possible multiple intersection. Since some limit had to be made on the number of diffracting planes investigated the six with the lowest Miller indices were chosen and the contribution made by these planes to multiple intersections was studied. Clearly if a Kossel curve is absent because its structure factor is zero it cannot participate in a multiple intersection. At the outset simple cubic, face and body centred cubic systems were studied. Then by variation of the lattice parameters in the computer data tetragonal and orthorhombic structures were also examined.

Some of the results are shown in Tables IV and V. The Miller indices of the diffracting planes which may participate in multiple intersections are listed. In Table IV the first three planes listed are (111) ($\bar{2}$00) ($\bar{3}$11) and clearly if we were dealing not with the (111) curve but the ($\bar{1}$11) curve the equivalent intersection would be between curves ($\bar{1}$11) (200) (311). Thus the intersections on other curves in the same family can be inferred. The letter T indicates that the intersection can persist if the crystal is tetragonal and the letter O that it also persists when the crystal is orthorhombic.

It should be noted that many of the multiple intersections are symmetrically related and these are next to one another in the tables. In fcc crystals, for example, (111) curves may have four sets of three symmetrically related multiple intersections. They are clearly in threes because [111] exhibits three-fold symmetry. When we turn to the (200) curves the intersections are in sets of four.

Quintuple intersections are seen in patterns from body centred cubic crystals, but these degenerate into pairs of triple intersections if the crystal becomes tetragonal. Orthorhombic crystals display markedly fewer multiple intersections than tetragonal which in turn have fewer than cubic crystals.

Turning to Fig. 1b and 1c again, we can now show how these tables are of use. Curves 4 and 14 surround a point of three fold symmetry and it has been shown that the crystal is face centred cubic in structure. Curve 4 is a (222) curve and exhibits three pairs of triple intersections in agreement with the number given in Table IV. The table indicates that the other curves participating in the intersections are from {200} and {220} planes. From curvature considerations the curve with least curvature in each case

TABLE IV Multiple intersections in face centred lattices (first six diffracting planes only)

{111} *lines*
(111) ($\bar{2}$00) ($\bar{3}$11) T
(111) (0$\bar{2}$0) (1$\bar{3}$1) T
(111) (00$\bar{2}$) (11$\bar{3}$)
(111) (2$\bar{2}$0) (3$\bar{1}$1)
(111) ($\bar{2}$20) ($\bar{1}$31)
(111) ($\bar{2}$02) ($\bar{1}$13)
(111) (02$\bar{2}$) (13$\bar{1}$)
(111) (0$\bar{2}$2) (1$\bar{1}$3)
(111) (20$\bar{2}$) (31$\bar{1}$)
(111) (311) (400) T.O.
(111) (131) (040) T.O.
(111) (113) (004) T.O.

{200} *lines*
(200) (020) (220) T.O.
(200) (002) (202) T.O.
(200) (0$\bar{2}$0) (2$\bar{2}$0) T.O.
(200) (00$\bar{2}$) (20$\bar{2}$) T.O.
(200) ($\bar{1}$11) (311) T.
(200) ($\bar{1}\bar{1}$1) (3$\bar{1}$1) T.
(200) ($\bar{1}$1$\bar{1}$) (31$\bar{1}$) T.
(200) ($\bar{1}\bar{1}\bar{1}$) (3$\bar{1}\bar{1}$) T.
(200) (02$\bar{2}$) (22$\bar{2}$)
(200) (0$\bar{2}$2) (2$\bar{2}$2)
(200) (0$\bar{2}\bar{2}$) (2$\bar{2}\bar{2}$)
(200) (022) (222)

{220} *lines*
(220) (1$\bar{1}$1) (311)
(220) ($\bar{1}$11) (131)
(220) (1$\bar{1}\bar{1}$) (31$\bar{1}$)
(220) ($\bar{1}$1$\bar{1}$) (13$\bar{1}$)
(220) (200) (020) T.O.
(220) (00$\bar{2}$) (22$\bar{2}$) T.O.
(220) (002) (222) T.O.
(220) (2$\bar{2}$0) (400) T.O.
(220) ($\bar{2}$20) (040) T.O.

{311} *lines*
(311) ($\bar{1}$11) (200) T.
(311) (1$\bar{1}$1) (220) T.
(311) (11$\bar{1}$) (202) T.
(311) (111) (400) T.O.

{222} *lines*
(222) (002) (220)
(222) (200) (022)
(222) (020) (202)

{400} *lines*
(400) (1$\bar{1}$1) (3$\bar{1}$1) T.O.
(400) (11$\bar{1}$) (31$\bar{1}$) T.O.
(400) (1$\bar{1}\bar{1}$) (3$\bar{1}\bar{1}$) T.O.
(400) (111) (311) T.O.
(400) (202) (20$\bar{2}$) T.O.
(400) (220) (2$\bar{2}$0) T.O.

TABLE V Multiple intersections in body centred systems (first six diffracting lines only)

Cubic	Tetragonal	Cubic	Tetragonal
{110} *lines*		{211} *lines*	
(110) (0$\bar{1}$1) (211) (1$\bar{1}$2) (202)	(110) (0$\bar{1}$1) 211)	(211) (110) (0$\bar{1}$1) (202) (1$\bar{1}$2)	(211) (110) (0$\bar{1}$1)
	(110) (1$\bar{1}$2) (202)	(211) (101) (01$\bar{1}$) (220) (12$\bar{1}$)	
(110) ($\bar{1}$01) (121) ($\bar{1}$12) (022)	(110) ($\bar{1}$01) (121)	(211) (011) (200)	T.O.
	(110) ($\bar{1}$12) (022)	(211) (0$\bar{1}\bar{1}$) (2$\bar{2}\bar{2}$)	T.O.
(110) ($\bar{1}$0$\bar{1}$) (12$\bar{1}$) ($\bar{1}$1$\bar{2}$) (02$\bar{2}$)	(110) ($\bar{1}$0$\bar{1}$) (12$\bar{1}$)	(211) ($\bar{1}$10) (031)	T.
	(110) ($\bar{1}$1$\bar{2}$) (02$\bar{2}$)	(211) ($\bar{1}$01) (013)	
(110) (0$\bar{1}\bar{1}$) (21$\bar{1}$) (1$\bar{1}\bar{2}$) (20$\bar{2}$)	(110) (0$\bar{1}\bar{1}$) (21$\bar{1}$)	(211) (20$\bar{2}$) (310)	
	(110) (1$\bar{1}\bar{2}$) (20$\bar{2}$)	(211) (2$\bar{2}$0) (301)	T.
(110) (0$\bar{2}$0) (1$\bar{3}$0) (310)	T.		
(110) ($\bar{2}$00) (130) ($\bar{3}$10)	T.	{220} *lines*	
(110) (1$\bar{1}$0) (200)	T.	(220) (101) (01$\bar{1}$) (12$\bar{1}$) (211)	
(110) ($\bar{1}$10) (020)	T.	(220) (011) (10$\bar{1}$) (121) (21$\bar{1}$)	
(110) (002) (112)	T.O.	(220) (1$\bar{1}$0) (310)	T.
(110) (00$\bar{2}$) (11$\bar{2}$)	T.O.	(220) ($\bar{1}$10) (130)	T.
(110) (1$\bar{2}$1) (301)	T.	(220) (200) (020)	T.O.
(110) ($\bar{2}$11) (031)	T.	(220) (00$\bar{2}$) (22$\bar{2}$)	T.O.
(110) (12$\bar{1}$) (30$\bar{1}$)	T.	(220) (002) (222)	T.O.
(110) ($\bar{2}$1$\bar{1}$) (03$\bar{1}$)	T.	(220) (2$\bar{1}$1) (301)	T.
(110) ($\bar{1}\bar{1}$2) (222)	T.O.	(220) (2$\bar{1}\bar{1}$) (30$\bar{1}$)	T.
(110) ($\bar{1}\bar{1}\bar{2}$) (22$\bar{2}$)	T.O.	(220) (031) ($\bar{1}$21)	T.
(110) (2$\bar{2}$0) (3$\bar{1}$0)	T.	(220) (03$\bar{1}$) ($\bar{1}$2$\bar{1}$)	T.
(110) ($\bar{2}$20) ($\bar{1}$30)	T.		
		{310} *lines*	
{200} *lines*		(310) (110) (0$\bar{2}$0) (1$\bar{3}$0	T.
(200) ($\bar{1}$10) (310) ($\bar{1}$30)	T.O.	(310) ($\bar{1}$10) (200) ($\bar{1}$30)	T.
(200) ($\bar{1}$01) (301) ($\bar{1}$03)	T.O.	(310) (101) (11$\bar{2}$)	
(200) ($\bar{1}\bar{1}$0) (3$\bar{1}$0) ($\bar{1}\bar{3}$0)	T.O.	(310) (10$\bar{1}$) (112)	
(200) ($\bar{1}$0$\bar{1}$) (30$\bar{1}$) ($\bar{1}$0$\bar{3}$)	T.O.	(310) (1$\bar{1}$0) (220)	T.
(200) (110) (1$\bar{1}$0)	T.	(310) (211) (20$\bar{2}$)	
(200) (101) (10$\bar{1}$)		(310) (21$\bar{1}$) (202)	
(200) (011) (211)	T.O.		
(200) (0$\bar{1}$1) (2$\bar{1}$1)	T.O.		
(200) (01$\bar{1}$) (21$\bar{1}$)	T.O.	{222} *lines*	
(200) (0$\bar{1}\bar{1}$) (2$\bar{1}\bar{1}$)	T.O.	(222) (211) ($\bar{2}$11) ($\bar{2}$22)	
(200) (020) (220)	T.O.	(222) (121) (1$\bar{2}$1) (2$\bar{2}$2)	
(200) (002) (202)	T.O.	(222) (112) (11$\bar{2}$) (22$\bar{2}$)	
(200) (0$\bar{2}$0) (2$\bar{2}$0)	T.O.	(222) (110) ($\bar{1}\bar{1}$2)	T.O.
(200) (00$\bar{2}$) (20$\bar{2}$)	T.O.	(222) (011) (2$\bar{1}\bar{1}$)	T.
(200) (022) (222)	T.O.	(222) (101) ($\bar{1}$2$\bar{1}$)	T.
(200) (02$\bar{2}$) (22$\bar{2}$)	T.O.	(222) (200) (022)	T.O.
(200) (0$\bar{2}$2) (2$\bar{2}$2)	T.O.	(222) (020) (202)	T.O.
(200) (0$\bar{2}\bar{2}$) (2$\bar{2}\bar{2}$)	T.O.	(222) (002) (220)	T.O.

will be from a {200} plane. Thus if curve 18 is (220) then curve 15 is (002) and if curve 16 is (020) then 20 is (202). Curves 17 and 19 must then be (200) and (022) respectively. Curve 18 also intersects with curves 2 and 8. Curve 8 being that with the next greatest curvature to curve 14 must be (3 1 1) and studying the table we see curve 2 must be (1 $\bar{1}$ 1). Study of the table reveals that in the absence of a (400) curve all the multiple intersections on the (220) curve have now been dealt with. Curve 20 makes a similar multiple intersection with curve 8 and from this we see in the table that curve 1 is (1 1 $\bar{1}$). The analysis continues in this manner and this method is the most rapid one for indexing cubic Kossel patterns.

6. Indexing in practice

The indexing techniques have been described with reference to a Kossel pattern from a face centred cubic crystal. This is a pattern that is easily solved by any of the methods given here.

Non-cubic crystals, however, exhibit Kossel patterns in which the indexing problem is more difficult and we will now demonstrate the application of the indexing techniques to the Kossel patterns from beryllium (hexagonal) and cementite (orthorhombic).

6.1. Beryllium

The pattern traced in Fig. 5 is a transmission pseudo-Kossel pattern from a beryllium crystal using Manganese radiation. Beryllium has a hexagonal crystal structure with lattice parameters, $a = 2.268$ Å, $c = 3.594$ Å (A.S.T.M.), and one would expect diffraction from the planes listed below in Table VI. In the figure there are three "mirror lines", XX′, YY′, ZZ′ which are traces of $(10\bar{1}0)$ $(11\bar{2}0)$ and (0002) planes. One mirror line, ZZ′, is at right angles to the other two and this must be a (0002) trace. Curves A and B are in the same zone and since they have the same axis perpendicular to ZZ′ this is the [0002] zone. From the Table VI we see that A and B can only be curves diffracted by the $\{10\bar{1}0\}$ and $\{1\bar{1}20\}$ famillies of planes and A having the greatest curvature is $\{1\bar{1}20\}$.

TABLE VI Diffraction from beryllium using manganese radiation

$(hkil)$	Intensity	α
$(10\bar{1}0)$	20	57° 46′
(0002)	14	54° 3′
$(10\bar{1}1)$	100	52° 36′
$(10\bar{1}2)$	12	37° 48′
$(11\bar{2}0)$	12	22° 48′

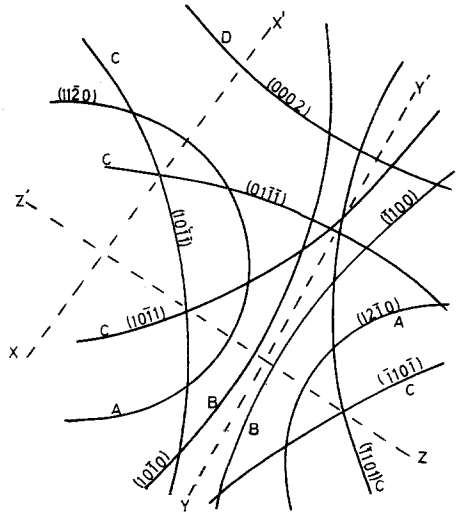

Figure 5 Beryllium Kossel pattern.

Curve D clearly has lines XX′ and YY′ as axes and must be (0002). Curve C can now only be $\{10\bar{1}1\}$ or $\{10\bar{1}2\}$. There is not sufficient curvature for the C curve to have a semi-apex angle of 37° 48′ (this is quickly seen, when Rowlands Bevis charts are used) and so they must be from planes of the $\{10\bar{1}1\}$ family. Curves from $\{10\bar{1}2\}$ planes were not detected in this pattern possibly because they were too weak to be seen.

6.2. Cementite

The crystal structure of cementite has been studied by many authors including Fasiska and Jeffrey [9] by Debye-Scherrer methods and is orthorhombic *Pnma*, with lattice parameters, $a = 4.525$ Å, $b = 5.088$ Å, $c = 6.740$ Å. Here the convention $a < b < c$ is used and our Miller indices differ in order from those of Fasiska and Jeffrey.

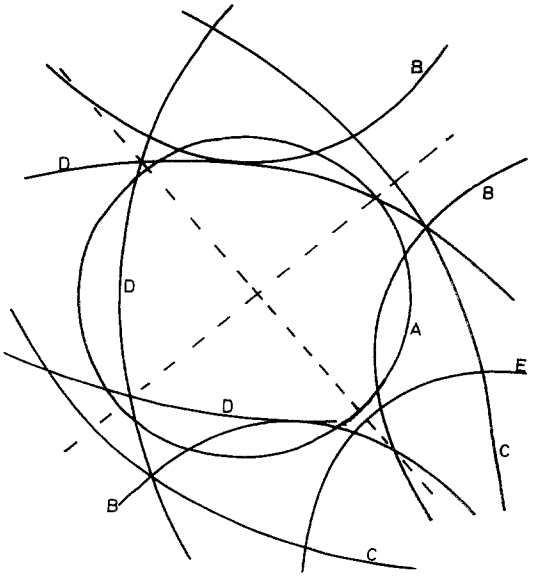

Figure 6 Cementite Kossel pattern.

Since the major elemental constituent is iron, the wavelength of the diffracted radiation is iron $K\alpha_1$, 1.935 Å. The drawing in Fig. 6 includes some but not all of the curves in the cementite Kossel pattern. Some curves were very weak and could not be discerned for much of their length. All the strongest curves are, however, included.

Preliminary study of the pattern indicates the presence of two "mirror lines" intersecting at

right angles. In our study of the symmetry we must allow for the non-appearance of some curves if other curves clearly indicate symmetry elements. The symmetry point at which the two lines intersect exhibits two-fold symmetry and is surrounded by the only full curve in the pattern. No geometrical multiple intersections are evident and because of low symmetry the method of counting intersections is unlikely to be successful. Two "accidental" multiple intersections are evident between curves C, B and D.

The symmetry point must indicate an axial direction and curve A clearly associated with this direction must have two Miller indices zero. The semi-apex angles α of the Kossel curves were determined by the Peters and Ogilvie method and are as follows:

$$A = 31°, B = 33°, C = 61°, D = 58° \text{ and } E = 28\tfrac{1}{2}°.$$

A list of possible Miller indices for A was drawn up from Fasiska and Jeffrrey's data and this is shown in Table VII. The only two sets of planes that could fit with the observed α angle of curve A are (400) and (006).

TABLE VII Cementite planes with two Miller indices zero

hkl	Structure factor	α
(200)	84.0	64° 40′
(400)	84.7	31° 12′
(004)	43.9	54° 57′
(006)	93.0	30° 30′

We now turn our attention to curves C and E which have mirror lines as their major axes and must have one Miller index zero since the lines are traces of (100) (010) or (001) planes. Again a list of planes with one Miller index zero was constructed and is given in Table VIII. Curves with structure factor below 50 have been excluded since one would not expect to detect them in the pattern.

TABLE VIII Cementite planes with one Miller index zero

hkl	Structure factor	α
(330)	115.8	44° 18′
(210)	109.4	62° 0′
(043)	104.2	29° 0′
(140)	93.3	37° 48′
(103)	114.3	61° 15′
(130)	78.4	52° 20′
(410)	83.5	23° 47′
(140)	93.3	37° 47′

Lattice planes producing curves with α angles similar to curve C are (103) and (210) and the only one corresponding with curve E is (043). The angle between the symmetry point and the [043] pole is found by the Peters and Ogilvie method and is 61°. This is in agreement with the angle between the [043] and [001] poles which means that the curve A must have indices (006) and in particular the symmetry point indicates an [001] direction. We may also conclude that because E is an (043) curve its axis must be the trace of a (100) plane and the other "mirror line" intersecting at right angles at the [001] pole is the trace of an (010) plane. Curves C must have Miller indices with $k = 0$ and are thus (103) and $(10\bar{3})$ Kossel curves. The angle between the poles of curves C and the [001] pole are in agreement with this conclusion. All other curves in the pattern may now be indexed according to the positions of their poles in the stereographic projection and following this course we find that curves D are diffracted by {113} planes and curves B by {233} planes.

7. Conclusion

Indexing procedures for Kossel patterns are unambiguous because symmetry, intensity, curvature, numbers of intersections, both simple and multiple and angles between poles in the stereographic projection must all support the result. So much information is available in a single Kossel pattern that it is an easy matter to cross-check the solution.

Much has been written about difficulties arising in the solution of powder patterns and diffractometric measurements. Many of these difficulties can be overcome by use of the back-reflection Kossel technique and this is clearly demonstrated in a study of tantalum oxide by Harris *et al.*[10].The volume of material required for these experiments is very much smaller than is required for powder patterns. A Kossel pattern may be obtained from a single crystal grain of material 5 μm in diameter. If the major elemental constituents of such a grain do not emit X-radiation of a suitable wavelength for diffraction by the crystal lattice this is overcome by the vacuum deposition of a $\frac{1}{2}$ μm thick layer of a suitable element on the surface of the crystal.

Few problems have been attempted in which Kossel diffraction is employed for the analysis of non-cubic crystal structures. It has been shown

that the indexing of Kossel patterns from cubic crystals is a simple matter but the indexing of patterns from non-cubic crystals is not a serious problem when all the indexing techniques are employed.

Acknowledgements

The author gratefully acknowledges the support of the Science Research Council for a research project of which this work is a part. The author also thanks Professor J. Stringer and members of the Department of Metallurgy and Materials Science, Liverpool University for their helpful discussion on the subject of this paper.

References

1. B. D. CULLITY, "Elements of X-ray Diffraction" (Adison Wesley, 1959).
2. P. C. ROWLANDS and M. F. BEVIS, *Phys. Stat. Sol* **26** (1968) K25.
3. E. T. PETERS and R. E. OGILVIE, *Trans. Met. Soc. AIME* **233** (1965) 89.
4. W. KOSSEL, *Ann. der Physik.* **25** (1936) 512.
5. K. J. H. MACKAY, "Proceedings of the Fourth Congress on X-ray Optics" (Hermann, Paris, 1966) p. 544.
6. J. Z. FRAZER and G. ARRHENIUS, *ibid* p. 516.
7. H. YAKOWITZ, *Adv. Electronics and Electron Phys. Suppl.* **6** (1969) 361.
8. K. LONSDALE, *Phil. Trans. Roy. Soc. Lond.* **A240** (1947) 219.
9. E. J. FASISKA and G. A. JEFFREY, *Acta Cryst.* **19** (1965) 463.
10. N. HARRIS, A. TAYLOR and J. STRINGER, *Acta Metallurgica* **21** (1973) 1677.

Received 22 July and accepted 29 July 1974.